However, at those frequencies the postfilter $P(D)$ can drastically remove it again. Thus, in Fig. 1 the data obtained by quantising $z_I(n)$ should be much less noisy compared to the data obtained by directly quantising $y_I(n)$. As the convergence of the CMA is in progress, the data received by the lower branch becomes more and more reliable and thus can be used in driving the LMS-type update algorithm. When the upper-branch CMA reaches its preset target performance, the switch (S/W) changes the position from 1 to 2. Then the lower branch governs the production of the final data estimate $\hat{b}(n)$ whereas the upper-branch CMA is in a waiting state by continuously updating its weights. When the underlying channel changes abruptly or the system fails and thus needs to restart, the S/W position goes from 2 back to 1. In general, some logic can be used to automatically control the S/W.

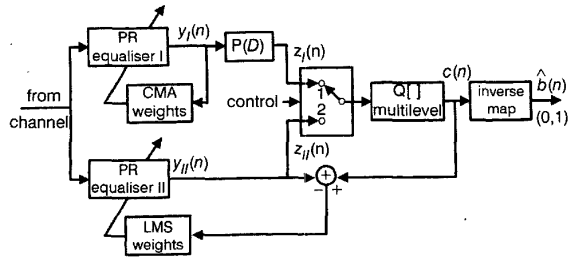

Fig. 1 *Proposed blind adaptive equalisation structure for precoded PR systems: CMA-LMS parallel structure*

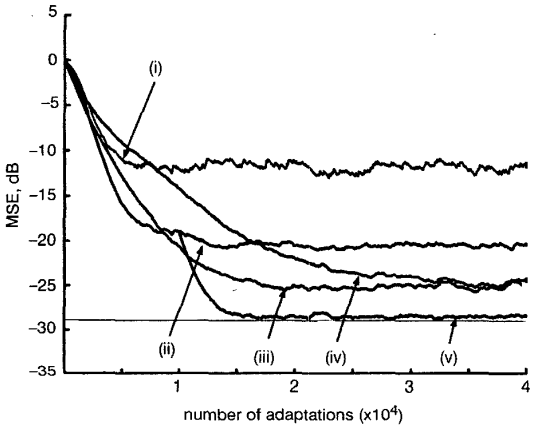

Fig. 2 *Comparison of data MSE $\hat{\varepsilon}_b$ for different blind adaptive equalisation methods*

Mode of operation changes at 10,000th input in all four cases
(i) Data MSE at CMA output
(ii) Simple CMA
(iii) CMA using generalised inverse prefilter ($\Delta = 0.05$)
(iv) CMA using pole-shifted inverse prefilter ($\alpha = 0.9$)
(v) Proposed CMA-LMS parallel structure

Performance comparison: To study the performance, we carried out computer simulation of a PR-IV system ($P(D) = 1 - D^2$) widely used in modelling the high-density magnetic recording system [3] where the pulse-width-50 parameter of the channel was set to 2.5 T. The SNR and the number of weights were 30 and 11 dB, respectively. Here, for comparison purposes we need to define a measure that is common to all the four cases. Unlike the general detection scheme shown in Fig. 1, for a PR-IV with binary input, one can alternatively obtain the estimate $\hat{b}(n)$ with binary quantisation performed last as $\hat{b}(n) = Q[|z(n)|/2]$, which prevents propagation of decision errors and is invariant to π (rad) phase shift. We then compute the normalised MSE $\varepsilon_b = E[\{b(n) - \hat{b}(n)\}^2]/E[\{b(n)\}^2]$. Fig. 2 shows the ensemble-averaged estimates for ε_b. It can be seen from the Figure that the use of the prefilters seems to work and improve the steady-state performance compared to the simple CMA. However, one can see further improvement obtained by the proposed structure. Note that even in the initial period that for the case of the simple CMA, $\hat{\varepsilon}_b$ denoted by (ii) and (v) decreases rapidly compared to the data MSE denoted by (i) corresponding to $y_I(n)$. The greatly decreased $\hat{\varepsilon}_b$ means that the postfilter successfully removes the error energy at the frequencies of the channel zeros and thus $\hat{b}(n)$ is sufficiently close to $b(n)$. Therefore, unlike $y_I(n)$, the postfilter output $z_I(n)$ contains a very reliable data reference. By updating the weights using this reference, the lower branch is getting ready for switching to obtain further improvement. After the S/Ws changes, the MSE $\hat{\varepsilon}_b$ decreases further by almost 8 dB. However, the reduction is not noticeable for the other three cases in which $Q[y_I(n)]$ is used as a data reference in the LMS-type weights update.

Concluding remarks: The approximations made to obtain the inverse filters of the prefilter-CMA approach result in insufficient MSE improvement and slower convergence. However, from the proposed structure we notice two distinct features: (1) A very reliable data reference can be derived initially using the postfilter; (2) The lower branch is equivalent in the steady state to the one that includes $P(D)$ in the equaliser weights, thus having the effect of almost completely cancelling the channel zeros on the unit circle. Therefore, the two branches have different achievable MSEs. This is why the proposed structure shows a dramatic improvement in performance. It can be seen that in the steady state $\hat{\varepsilon}_b$ becomes very close to the theoretical/calculated minimum MSE of -28.68 dB. A detailed study of convergence is under way although high-order analysis is involved therein.

Acknowledgement: This work was supported by Korea Research Foundation Grant (KRF-99-041-E00232).

25 June 2001
Electronics Letters Online No: 20020063
DOI: 10.1049/el:20020063

Jae-Chon Lee (*Department of Systems Engineering, Ajou University, P.O. Box 25, Yong-In-Si, Kyong-Gi-Do, Zip 449-820, Korea*)

E-mail: jaelee@ajou.ac.kr

References

1 JOHNSON, C.R. JR., SCHNITER, P., ENDRES, T.J., BEHM, J.D., BROWN, D.R., and CASAS, R.A.: 'Blind equalization using the constant modulus criterion: a review', *Proc. IEEE*, 1998, **86**, pp. 1927–1950
2 PROAKIS, J.G.: 'Digital communications' (McGraw Hill, New York, 1989, 2nd edn.), pp. 528–548
3 CIOFFI, J.M., ABBOTT, W.L., THAPAR, H.K., MELAS, C.M., and FISHER, K.D.: 'Adaptive equalization in magnetic-disk storage channels', *IEEE Commun. Mag.*, 1990, pp. 14–29
4 TUGNAIT, J.K., and GUMMADAVELLI, U.: 'Blind equalization and channel estimation with partial response input signals', *IEEE Trans. Commun.*, 1997, **45**, pp. 1025–1031

Fast adaptation of fractionally spaced equalisers

H. Mohamad, S. Weiss, M. Rupp and L. Hanzo

Efficient subband structures that aim at fast adaptation of fractionally spaced equalisers (FSE), by exploiting the 'prewhitening' effect that a subband decomposition has on the spectral dynamics of the equaliser input are discussed. Two novel FSE structures are proposed, which differ in the extent to which the feed-forward and feed-back sections of the FSE are implemented in the subband domain, with distinct impacts on the updating. Improved convergence is achieved at a reduced computational cost compared to a fullband benchmark.

Introduction: Fractionally spaced equalisers (FSE) have been widely applied for combatting intersymbol interference (ISI) in communication systems due to their improved performance as compared to their symbol spaced counterparts [1]. However, it has been shown that due to the colouring imposed by the channel, the eigenvalue spread of the FSE input may significantly reduce the convergence speed of least mean squares (LMS) type algorithms [2]. Therefore, in this Letter we aim to improve this convergence behaviour, while retaining the benefits of low complexity when using the LMS algorithm.

A subband decomposition 'prewhitens' the signals and therefore has been employed for example in acoustic echo cancellation to improve the LMS convergence [3]. Hence in this Letter, we propose two different novel subband structures for FSEs to enhance their convergence rate, whereby the focus is on adaptation with an explicit training signal.

Fractionally spaced equaliser structure: The schematic diagram of the FSE is shown in Fig. 1. The feed-forward (FF) part is operating at twice the symbol rate and implemented as a polyphase structure [4] having partial responses $a_0[n]$ and $a_1[n]$. A feed-back (FB) filter $b[n]$ running at symbol rate is also included in the structure of Fig. 1. For updating, the normalised LMS (NLMS) algorithm can be applied in an equation-error IIR multichannel adaptive filter structure [5], whereby a delayed copy of the transmitted signal $u[n]$ is available as a training sequence $d[n]$ at the receiver.

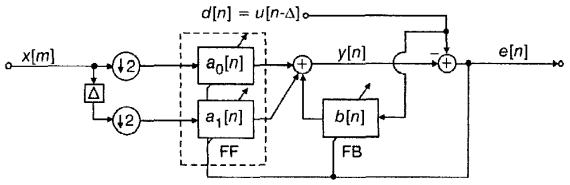

Fig. 1 *Fullband FSE in polyphase realisation*

The spectral dynamics, and therefore the large eigenvalue spread, of the FSE's oversampled input signal $x[m]$ results in a considerably reduced convergence speed for the filters $a_0[n]$ and $a_1[n]$. As the FB section is excited by the original symbol sequence, which is generally scrambled and therefore uncorrelated, the convergence of the filter $b[n]$ is unaffected by this phenomenon.

Subband structures: In a subband system, a fullband signal is decomposed into K frequency bands decimated by a factor of N by means of an analysis filter bank [3, 4]. In the following section, this operation will be denoted by **H**. In a dual operation, a synthesis filter bank denoted by **G** reconstructs a fullband signal from the subbands. Owing to the separation into narrow spectral intervals, the subband signals are generally whitened and therefore permit faster adaptation, when an LMS-type adaptive filter is applied independently in each subband compared to the fullband domain [3]. For such subband adaptive systems, oversampling with $N<K$ is chosen to limit the effect of aliasing within the subbands on the convergence [6].

If only the FF part of the fullband equaliser in Fig. 1 is projected into subbands, the architecture (structure I) shown in Fig. 2 results. The system blocks $\mathbf{A}_0$ and $\mathbf{A}_1$ contain the coefficients of the adaptive filters which are operated independently in the K subbands. The error $e[n]=d[n]-y[n]$ is evaluated in the fullband after reconstruction by **G**, and projected back into the subband domain to update the filters described by $\mathbf{A}_0$ and $\mathbf{A}_1$.

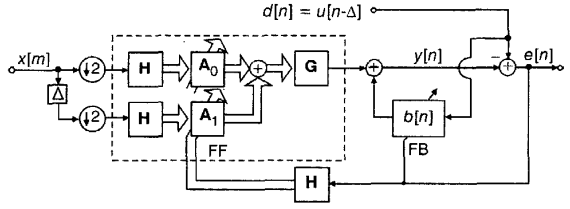

Fig. 2 *Subband FSE structure I*

While prewhitening of the subband signals in the FF part is established, the delay imposed by the filter banks on the algorithm update requires the use of delay-LMS type algorithms, which are prone to degrade adaptation speed [7]. To circumvent this problem, the FSE's FB part can also be implemented in subbands, as shown in Fig. 3 (structure II). The block **B** contains independent adaptive filters applied to each subband, similarly, to the definition of $\mathbf{A}_0$ and $\mathbf{A}_1$. Note, that in structure II no delays exist in the error paths and all adaptive filters in $\mathbf{A}_0$, $\mathbf{A}_1$ and $\mathbf{B}_0$ are updated with the same subband error signals at the same time, which is expected to lead to a more balanced convergence of the different FSE sections.

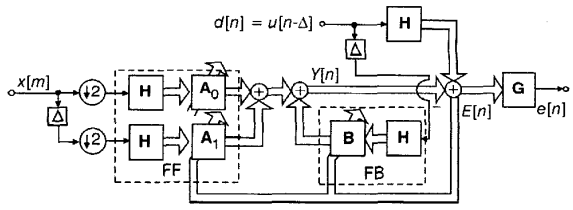

Fig. 3 *Subband FSE structure II*

Simulation results: A severely dispersive Gaussian channel having a delay spread of approximately 100 symbol periods and spectral zeros was employed for testing the performance of the different FSE structures in conjunction with 64-QAM modulation for signal transmission. The channel exhibited an SNR of 20 dB. The fullband FSE used 500 and 100 coefficients in the FF and FB parts, respectively. In all cases, the NLMS algorithm having a step size of $\tilde{\mu}=0.4$ was employed. The delay Δ was selected such that the FF-part of the FSE mainly acted on the pre-cursor ISI. For structures I and II, filter banks with $K=16$ subbands decimated by $N=14$ were employed. Owing to the increased sampling period in the subbands, the order of subband-based FSE sections can be reduced by approximately a factor of N without impairing the steady-state mean square error (MSE) performance [6].

The MSE curves for the three different FSE structures are shown in Fig. 4, after averaging over 20 ensemble runs. The graphs show a general advantage for the subband FSE structures in adaptation speed, whereby structure II exhibits the best initial convergence speed amongst the three. An overall faster convergence of subband FSE structures is observed in comparison to the fullband realisation, which can be attributed to the prewhitening effect of the subband decomposition of the FF section.

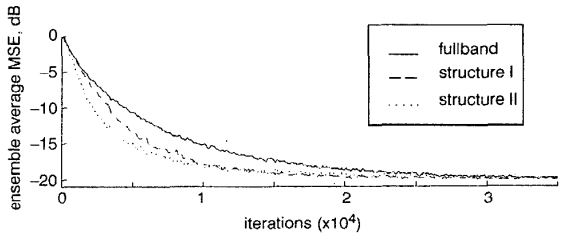

Fig. 4 *MSE curves for FSE structures of Figs. 1–3*

To explore the adaptation behaviour of the different FSE sections, the transient behaviour of the largest coefficients of both FF sections and that of the FB section has been recorded. The moduli of these coefficients are displayed in Fig. 5, normalised with respect to their steady-state value. Since the two FF sections only insignificantly varied from each other, they are only given as a single averaged curve. It is observed in Fig. 5 that for structure I the FF and FB sections show a considerable difference in terms of their convergence, whereby the slower FB part limits the overall adaptation speed. For structure II the convergence speed of the FB part was increased. Since in this case the eigenvalue spread of the FB input was not improved over structure I, the faster convergence is likely to be due to the improved updating procedure based on the same error subband signals.

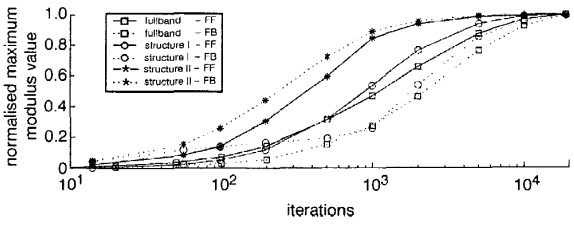

Fig. 5 *Maximum normalised coefficient moduli*

In addition to their increased convergence speed, the subband structures I and II only require 37% and 29% of the fullband FSE's computational complexity, respectively, due to their proportionately reduced filter orders.

Conclusion: Subband decompositions have been proposed to overcome the slow convergence of FSEs. Two different subband-based FSE structures have been studied. Our simulations suggest that both structures provide an enhanced convergence rate, whereby structure II with a subband realisation of both FF and FB sections has been identified as the superior system. An additional appeal of the proposed structures is their reduced computational cost.

21 November 2001
Electronics Letters Online No: 20020064
DOI: 10.1049/el:20020064

H. Mohamad, S. Weiss and L. Hanzo (*Department of Electronic and Computer Science, University of Southampton, Highfield, Southampton SO17 1BJ, United Kingdom*)

E-mail: hm99r@ecs.soton.ac.uk

M. Rupp (*Wireless Technology Research Department, Lucent Technologies, Bell Laboratories, Holmdel, NJ 07733, USA*)

References

1 QURESHI, S.U.H.: 'Adaptive equalization', *Proc. IEEE*, 1985, **73**, pp. 1349–1387
2 RUPP, M.: 'On the learning behaviour of decision feedback equalizers'. Proc. 33rd Asilomar Conf. on Signals, Systems, and Computers, 1999, Vol. 1, pp. 514–518
3 KELLERMANN, W.: 'Analysis and design of multirate systems for the cancellation of acoustical echoes'. Proc. ICASSP, 1998, Vol. 3, pp. 2570–2573
4 VAIDYANATHAN, P.P.: 'Multirate systems and filter banks' (Prentice Hall, 1993)
5 SHYNK, J.J.: 'Frequency-domain and multirate adaptive filtering', *IEEE Signal Process. Magazine*, 1992, **9**, pp. 14–37
6 WEISS, S., STENGER, A., STEWART, R.W., and RABENSTEIN, R.: 'Steady-state performance limitations of subband adaptive filters', *IEEE Trans. Signal Process.*, 2001, **49**, (9), pp. 1982–1991
7 RUPP, M., and FRENZEL, R.: 'Analysis of LMS and NLMS algorithms with delayed coefficient update under the presence of spherically invariant processes', *IEEE Trans. Signal Process.*, 1994, **42**, (3), pp. 668–672

Spectral reconfiguration, permutation and mapping

R.A. King and A. Clifton

A new method of improving the performance of Fourier-based signal processing systems is presented. The method is simple to embody and is shown to have wide application.

Background: Throughout the last five to six decades, the Fourier transform, its digital offspring and their inverses have provided engineers and scientists with key enabling tools over a very wide range of application areas. In 1948, Claude Shannon's celebrated work on information theory [1] set mathematical bounds on the nature of human communication. This was followed in 1949 by his sampling theorem [2], specifying a minimum requirement of 2TW independent numbers to describe any band-limited function of time T and bandwidth W. These mathematical constructs provide the basis for the majority of present day analogue and digital data transmission, signal processing and signal characterisation systems.

Zero-based coding concepts: In 1958 and 1960, Bond and Cahn [3, 4] suggested an alternative theoretical approach to signal coding, which relied on the work of Levin [5]. They proposed the real and complex 'zeros' of a waveform as its information bearing attributes. In 1966, this mathematical option was promoted by Voelcker [6] in search of a universal theory of modulation. The mathematics throughout were unusual and formidable. Furthermore, the search for mathematical completeness indicated a need for procedures that appeared computationally infeasible. As a result, little serious attention was paid to this approach.

Time encoded speech and time encoded signal processing and recognition: In 1978, a Letter by King and Gosling, 'Time encoded speech' (TES) [7], described an application of the disclosures of Bond and Cahn to the development of a 'zero based' model of human speech. This model utilised 'coded shape descriptors' of the speech waveform, based upon approximations to the locations and rankings of its real and complex zeros. By these means, simple fixed dimension matrix models were used as classification entities suitable for characterisation and comparison by conventional classical correlation routines or by artificial neural network means. These (TES) disclosures and subsequent developments, which extended zero-based concepts to all band-limited waveforms, i.e. time encoded signal processing and recognition (TESPAR), are summarised in [8].

Waveform shape descriptors and 2TW Shannon samples: Work since 1978 has promoted the use of 'waveform shape descriptors' (WSDs) such as TES and TESPAR as highly effective representations for all band-limited waveforms. By these means, successive quantised and coded 'shape descriptors' of a waveform under investigation provide the ensemble of (2TW) Shannon numbers required to describe it [8]. Other non-TESPAR WSD systems subsequently offered for signal characterisation include those of the University of Wales [9], Omron [10] and a number of wavelet transform variants.

WSDs and the Fourier transform: The Fourier transform (FT) may be applied to all band-limited functions (waveforms) including random functions. The transform may be analogue or digital to produce spectral representations which take different forms. For the purpose of this Letter, only the 'spectral plot' (SP) which provides spectral 'location', 'magnitude' and 'phase' information will be discussed. For clarity, the discrete Fourier transform (DFT) and its inverse (the IDFT), will be used to illustrate key concepts associated with the spectral reconfiguration, permutation and mapping (SRP&M) philosophy which follows.

Spectral plot, WSDs and SRP&M: A band-limited signal under test (SUT) comprising '2N' sampled signal ordinate values will, via the DFT, produce a spectral plot (SP), i.e. a numerical measure of magnitude and phase for each of the 'N' positive spectral locations. Application of the IDFT, by any conventional means, will enable the waveform of the original SUT to be reconstructed, to a specified precision, from its original spectral plot. What has now been confirmed is that the performance of all characterisation and classification systems utilising FTs and WSDs is tractable to a range of productive SRP&Ms that may, by means of the procedures described below, enable very difficult characterisations to be achieved which might otherwise be considered unattainable.

Fig. 1 is a block diagram of a typical WSD coding and classification system. Fig. 2 shows a block diagram of a WSD coding system invoking SRP&M. As indicated, after DFT processing, all the signals under test have their spectral entities subjected to an identical SRP&M. The spectral plots so modified are then converted back to waveforms by means of an IDFT. The resulting modified waveforms are passed to the WSD coder, and thence for classification, by standard WSD means. Thus the reconstructed waveforms of each of the SUTs after SRP&M are available as new informative versions of the original signals for subsequent WSD coding and classification purposes.

The SRP&M may take any consistent form. For example, one to one, one to many, many to one, mappings; linear, nonlinear, random or functional reconfigurations; or combinations of such, provided always, that any such SRP&M is applied identically to some or all of the elements of each of the individual SPs of the signals under test. It will be clear that a very large number of different SRP&M transformations are available. For example, if random permutations are to be applied to the linked magnitude and phase vectors of an SP of 'N' positive elements, the number of different SRP&M options available is 'N!'. Practically, near optimum SRP&Ms are currently being identified via random search procedures. Typically, given two representative sets of 12 SUTs, searches of 10,000 iterations produce five, or six, effective SRP&M candidates in 5 to 6 h on an 800 MHz Pentium III processor. We find that engineering judgement can often bypass the tedium of random processing.

The methods described have been validated on widely differing waveform sets and application areas. WSDs investigated and found suitable include TES and TESPAR [8], the University of Wales algorithm